Search for heavy resonances decaying into a pair of Z bosons with the ATLAS detector

Joey Carter

University of Toronto

June 7, 2021

Motivation: Multiple Higgs bosons?

- Measurements of the Higgs boson at the LHC have shown excellent agreement with Standard Model (SM) predictions:
  - → Production cross sections, branching ratios, couplings to vector bosons and fermions.

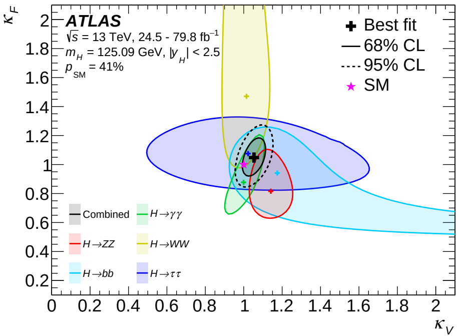

Phys. Rev. D **101** (2020) 012002

Motivation: Multiple Higgs bosons?

- Measurements of the Higgs boson at the LHC have shown excellent agreement with Standard Model (SM) predictions:
  - → Production cross sections, branching ratios, couplings to vector bosons and fermions.

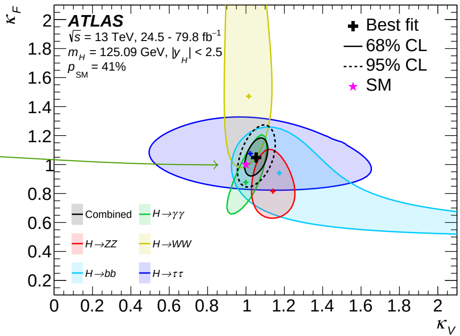

Phys. Rev. D **101** (2020) 012002

Motivation: Multiple Higgs bosons?

- Measurements of the Higgs boson at the LHC have shown excellent agreement with Standard Model (SM) predictions:
  - → Production cross sections, branching ratios, couplings to vector bosons and fermions.
- The SM is not the ultimate theory of nature and has many well-documented shortcomings:
  - → No explanation of gravity, matter-antimatter asymmetry; no dark matter candidate; neutrino masses not included; the *hierarchy problem* and questions of Higgs mass "naturalness"...

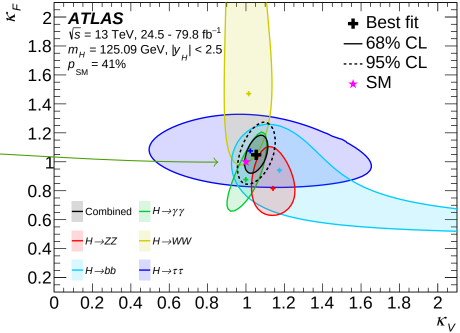

Phys. Rev. D **101** (2020) 012002

Motivation: Multiple Higgs bosons?

- Measurements of the Higgs boson at the LHC have shown excellent agreement with Standard Model (SM) predictions:
  - → Production cross sections, branching ratios, couplings to vector bosons and fermions.
- The SM is not the ultimate theory of nature and has many well-documented shortcomings:
  - → No explanation of gravity, matter-antimatter asymmetry; no dark matter candidate; neutrino masses not included; the *hierarchy problem* and questions of Higgs mass "naturalness"...

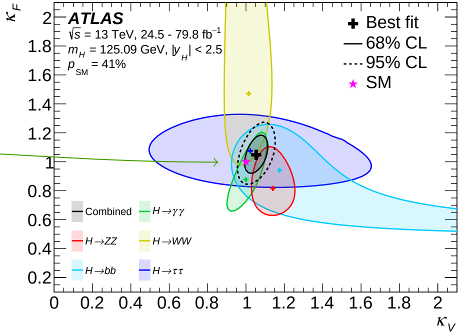

Phys. Rev. D **101** (2020) 012002

Many extensions of the Standard Model predict additional Higgs bosons

- For example, **Two-Higgs-doublet models** (2HDM) predict 5 Higgs bosons: two neutral CP even (h, H), one CP odd (A) and two charged Higgs bosons ($H^{\pm}$).

Motivation: Multiple Higgs bosons?

- Measurements of the Higgs boson at the LHC have shown excellent agreement with Standard Model (SM) predictions:
  - → Production cross sections, branching ratios, couplings to vector bosons and fermions.
- The SM is not the ultimate theory of nature and has many well-documented shortcomings:
  - → No explanation of gravity, matter-antimatter asymmetry; no dark matter candidate; neutrino masses not included; the *hierarchy problem* and questions of Higgs mass "naturalness"…

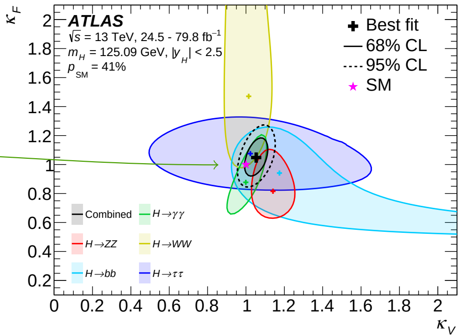

Phys. Rev. D **101** (2020) 012002

Many extensions of the Standard Model predict additional Higgs bosons

- For example, **Two-Higgs-doublet models** (2HDM) predict 5 Higgs bosons: two neutral CP even (h, H), one CP odd (A) and two charged Higgs bosons ($H^{\pm}$).
  - → The Minimal Supersymmetric Standard Model (MSSM) is one such 2HDM model.

The ATLAS Higgs-like search program

JINST 3 (2008) S08003

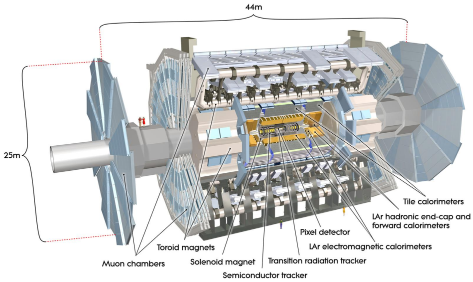

The ATLAS Experiment at the LHC

- General-purpose detector at the Large Hadron Collider.
- Recorded 139 fb^{-1} of *pp* collision data at $\sqrt{s} = 13\,\mathrm{TeV}$ during Run 2 of the LHC.

The ATLAS Higgs-like search program

JINST 3 (2008) S08003

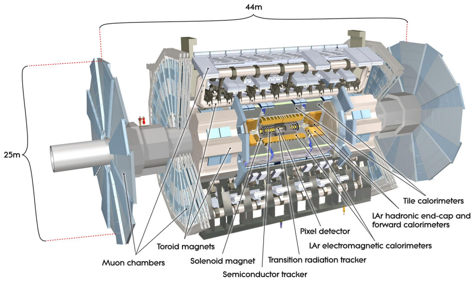

The ATLAS Experiment at the LHC

- General-purpose detector at the Large Hadron Collider.
- Recorded 139 fb^{-1} of pp collision data at $\sqrt{s} = 13\,\mathrm{TeV}$ during Run 2 of the LHC.

Method 1 | Indirect Searches, e.g.:

- Precision measurements of SM Higgs couplings and reinterpretations in BSM extensions.
- Searches for DM with interpretations in models with extended Higgs sector.

The ATLAS Higgs-like search program

JINST 3 (2008) S08003

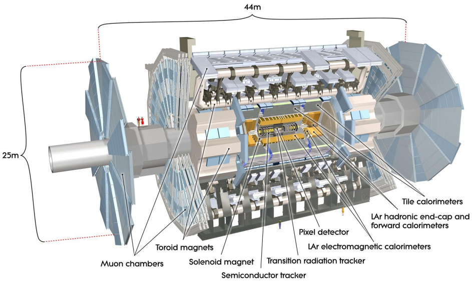

The ATLAS Experiment at the LHC

- General-purpose detector at the Large Hadron Collider.
- Recorded 139 fb^{-1} of pp collision data at $\sqrt{s} = 13$ TeV during Run 2 of the LHC.

Method 1 | Indirect Searches, e.g.:

- Precision measurements of SM Higgs couplings and reinterpretations in BSM extensions.
- Searches for DM with interpretations in models with extended Higgs sector.

Method 2 | Direct Searches:

- Searches for additional neutral Higgs bosons and other heavy diboson resonances in “most likely” final states.
- ATLAS also active in searches for singly- and doubly-charged Higgs bosons, and searches for resonant di-Higgs production.

The ATLAS Higgs-like search program

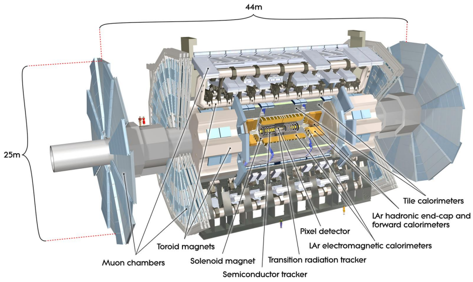

JINST 3 (2008) S08003

The ATLAS Experiment at the LHC

- General-purpose detector at the Large Hadron Collider.
- Recorded 139 fb^{-1} of pp collision data at $\sqrt{s} = 13$ TeV during Run 2 of the LHC.

Method 1 | Indirect Searches, e.g.:

- Precision measurements of SM Higgs couplings and reinterpretations in BSM extensions.
- Searches for DM with interpretations in models with extended Higgs sector.

Method 2 | Direct Searches:

- Searches for additional neutral Higgs bosons and other heavy diboson resonances in "most likely" final states.
- ATLAS also active in searches for singly- and doubly-charged Higgs bosons, and searches for resonant di-Higgs production.

Focus of this talk
Searches for $X \to ZZ$

Searches for heavy ZZ resonances

Eur. Phys. J. C **81** (2021) 332

Search for heavy spin-0 (heavy Higgs) and spin-2 (graviton) resonances with full Run 2 dataset

- Combination of 4ℓ and $\ell\ell\nu\nu$ channels:
  - → Benefit from mass resolution of 4ℓ and larger branching ratio of $\ell\ell\nu\nu$.
- Improves upon previous ATLAS search at $\sqrt{s} = 13\,\text{TeV}$ using $36.1\,\text{fb}^{-1}$ (from 2015+16)
  - → Eur. Phys. J. C **78** (2018) 293
  - → Observed two excesses of $\sim 2.5\sigma$ global significance in 4ℓ channel at ~ 240 and 700 GeV, none in $\ell\ell\nu\nu$.
- General analysis improvements:
  - → Increased luminosity → larger dataset
  - → Improved lepton reconstruction/isolation and use of particle-flow jets
  - → Improved background modelling → extend search range up to 2 TeV
  - → Improved event selection in $\ell\ell\nu\nu$ channel
  - → Use of Neural Network (NN) for event classification in 4ℓ channel

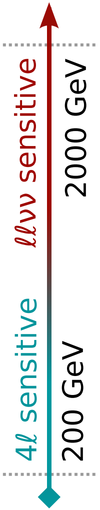

$ZZ \to 4\ell$ Analysis

Selections, Event Categorization and Signal Modelling

- Select **two** same-flavour, opposite-sign lepton pairs ($\ell = e, \mu$).
  - → Three final states: 4μ, $4e$, and $2\mu 2e$.
  - → Select only isolated leptons sharing a common vertex.

Selections, Event Categorization and Signal Modelling

- Select **two** same-flavour, opposite-sign lepton pairs ($\ell = e, \mu$).
  - Three final states: 4μ, $4e$, and $2\mu 2e$.
  - Select only isolated leptons sharing a common vertex.
- Event categorization by **two separate neural networks**: one classifier for ggF and one for VBF:
  - 5 event categories depending on jet multiplicity and NN score (with *ggF-MVA-high* subdivided by lepton flavour).

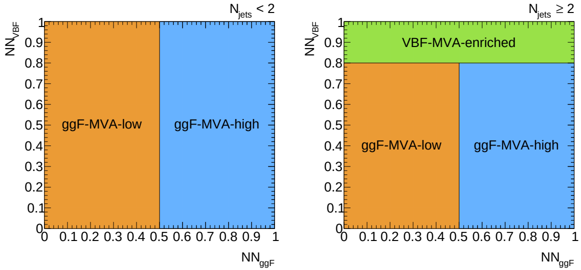

Selections, Event Categorization and Signal Modelling

- Select **two** same-flavour, opposite-sign lepton pairs ($\ell = e, \mu$).
  - Three final states: 4μ, $4e$, and $2\mu 2e$.
  - Select only isolated leptons sharing a common vertex.
- Event categorization by **two separate neural networks**: one classifier for ggF and one for VBF:
  - 5 event categories depending on jet multiplicity and NN score (with *ggF-MVA-high* subdivided by lepton flavour).

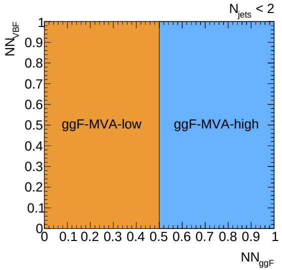

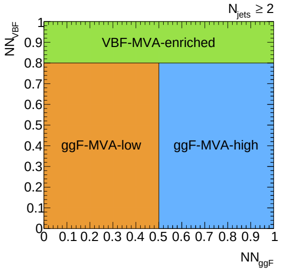

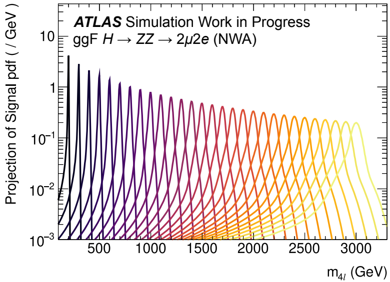

- Narrow-width approximation (**NWA**): signal $m_{4\ell}$ shape parameterized in each 4ℓ final state from fit to MC simulation.

Selections, Event Categorization and Signal Modelling

- Select **two** same-flavour, opposite-sign lepton pairs ($\ell = e, \mu$).
  - → Three final states: 4μ, $4e$, and $2\mu 2e$.
  - → Select only isolated leptons sharing a common vertex.
- Event categorization by **two separate neural networks**: one classifier for ggF and one for VBF:
  - → 5 event categories depending on jet multiplicity and NN score (with *ggF-MVA-high* subdivided by lepton flavour).

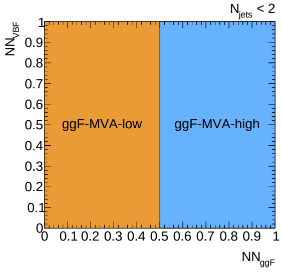

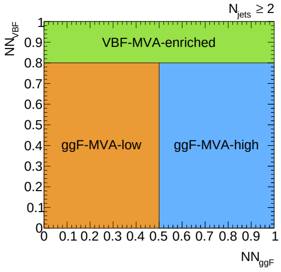

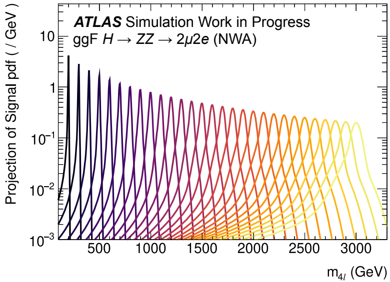

- Narrow-width approximation (**NWA**): signal $m_{4\ell}$ shape parameterized in each 4ℓ final state from fit to MC simulation.
- Large-width assumption (**LWA**): parton-level lineshape $\otimes$ detector resolution (interference effects accounted for).

Backgrounds

Irreducible Backgrounds

- **Main background** from non-resonant ZZ ($\sim$97 % of total background events):
  - → $q\bar{q} \to ZZ$
  - → $gg \to ZZ$
  - → EW vector-boson scattering ($ZZjj$, mostly in VBF category)
- Shape modelled by empirical function, normalization allowed to vary freely in fit to data.

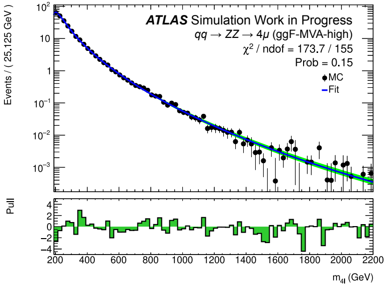

Backgrounds

Irreducible Backgrounds

- **Main background** from non-resonant ZZ ($\sim$97 % of total background events):
  - → $q\bar{q} \to ZZ$
  - → $gg \to ZZ$
  - → EW vector-boson scattering ($ZZjj$, mostly in VBF category)
- Shape modelled by empirical function, normalization allowed to vary freely in fit to data.

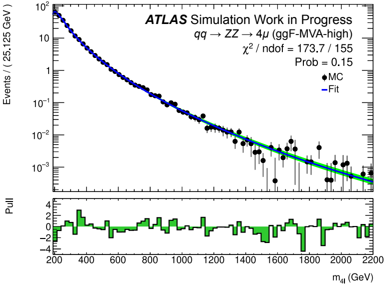

EPJC 80 (2020) 957

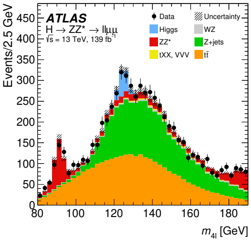

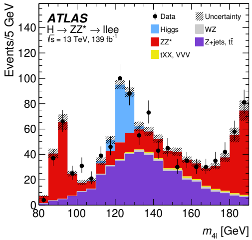

*Example of $\ell\ell + \mu\mu$ and $\ell\ell + ee$ control regions from SM Higgs analysis

Reducible Backgrounds

- Z+jets and $t\bar{t}$ ($\sim$ 1 % of expected backgrounds):
  - → Estimated using data-driven methods in dedicated $\ell\ell + \mu\mu$ and $\ell\ell + ee$ control regions.
- $t\bar{t}V$ and VVV (< 1 % of expected backgrounds):
  - → Shape and normalization directly from MC.

Results

- Neural network outputs show good performance of categorization system. →
- Good agreement between data and background-only predictions over full mass range in all categories.
  - → **No significant excesses observed.**

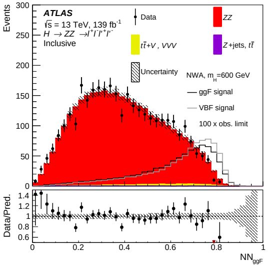

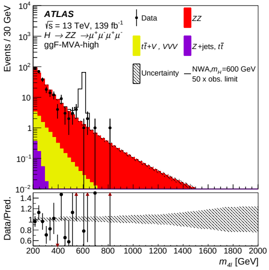

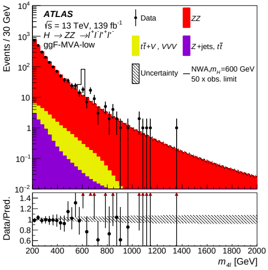

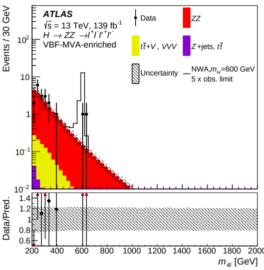

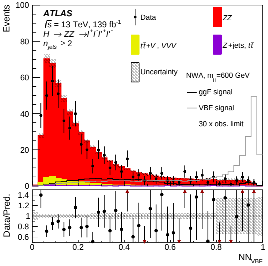

EPJC 81 (2021) 332

$ZZ \to \ell\ell\nu\nu$ Analysis

Selections, Event Categorization and Backgrounds

- Select **one** same-flavour, opposite-sign lepton pair + $E_{\mathrm{T}}^{\mathrm{miss}}$.
  - → Require $E_{\mathrm{T}}^{\mathrm{miss}} > 120\,\mathrm{GeV}$ and **high $E_{\mathrm{T}}^{\mathrm{miss}}$ significance**.
  - → Also require $E_{\mathrm{T}}^{\mathrm{miss}}$ to be back-to-back with lepton pair: $\Delta\phi(\vec{p}_{\mathrm{T}}^{\,\ell\ell}, \vec{E}_{\mathrm{T}}^{\mathrm{miss}}) > 2.5\,\mathrm{rad}$

Selections, Event Categorization and Backgrounds

- Select **one** same-flavour, opposite-sign lepton pair + $E_{\mathrm{T}}^{\mathrm{miss}}$.
  - → Require $E_{\mathrm{T}}^{\mathrm{miss}} > 120\,\mathrm{GeV}$ and **high $E_{\mathrm{T}}^{\mathrm{miss}}$ significance**.
  - → Also require $E_{\mathrm{T}}^{\mathrm{miss}}$ to be back-to-back with lepton pair: $\Delta\phi(\vec{p}_{\mathrm{T}}^{\,\ell\ell}, \vec{E}_{\mathrm{T}}^{\mathrm{miss}}) > 2.5\,\mathrm{rad}$
- Full invariant mass cannot be reconstructed → use **transverse mass** as discriminating variable:

$$m_{\mathrm{T}} \equiv \sqrt{\left[\sqrt{m_Z^2 + \left(p_{\mathrm{T}}^{\ell\ell}\right)^2} + \sqrt{m_Z^2 + \left(E_{\mathrm{T}}^{\mathrm{miss}}\right)^2}\,\right]^2 - \left|\vec{p}_{\mathrm{T}}^{\,\ell\ell} + \vec{E}_{\mathrm{T}}^{\mathrm{miss}}\right|^2}$$

Selections, Event Categorization and Backgrounds

- Select **one** same-flavour, opposite-sign lepton pair + $E_{\mathrm{T}}^{\mathrm{miss}}$.
  - Require $E_{\mathrm{T}}^{\mathrm{miss}} > 120\,\mathrm{GeV}$ and **high $E_{\mathrm{T}}^{\mathrm{miss}}$ significance**.
  - Also require $E_{\mathrm{T}}^{\mathrm{miss}}$ to be back-to-back with lepton pair: $\Delta\phi(\vec{p}_{\mathrm{T}}^{\ell\ell}, \vec{E}_{\mathrm{T}}^{\mathrm{miss}}) > 2.5\,\mathrm{rad}$
- Full invariant mass cannot be reconstructed → use **transverse mass** as discriminating variable:

$$m_{\mathrm{T}} \equiv \sqrt{\left[\sqrt{m_Z^2 + \left(p_{\mathrm{T}}^{\ell\ell}\right)^2} + \sqrt{m_Z^2 + \left(E_{\mathrm{T}}^{\mathrm{miss}}\right)^2}\right]^2 - \left|\vec{p}_{\mathrm{T}}^{\ell\ell} + \vec{E}_{\mathrm{T}}^{\mathrm{miss}}\right|^2}$$

- Use **cut-based approach** to categorize ggF-like and VBF-like events:
  - VBF-like if $m_{jj} > 550\,\mathrm{GeV}$, $\Delta\eta_{jj} > 4.4$

Background Modelling and Results

- **Dominant backgrounds** from ZZ and WZ:
  - → ZZ from simulation with floating normalization.
  - → WZ estimated using data-driven method with 3-lepton control region.

Background Modelling and Results

- **Dominant backgrounds** from ZZ and WZ:
  - → ZZ from simulation with floating normalization.
  - → WZ estimated using data-driven method with 3-lepton control region.
- **Small background contributions** from $Z(\to ee, \mu\mu)$+jets and WW/top/$Z \to \tau\tau$
  - → Estimated using data-driven methods in dedicated control regions.

Background Modelling and Results

- **Dominant backgrounds** from ZZ and WZ:
  - → ZZ from simulation with floating normalization.
  - → WZ estimated using data-driven method with 3-lepton control region.
- **Small background contributions** from $Z(\to ee, \mu\mu)$+jets and WW/top/$Z \to \tau\tau$
  - → Estimated using data-driven methods in dedicated control regions.
- **Results:** Good agreement between data and background-only predictions in all categories.
  - → **No significant excess observed.**

EPJC 81 (2021) 332

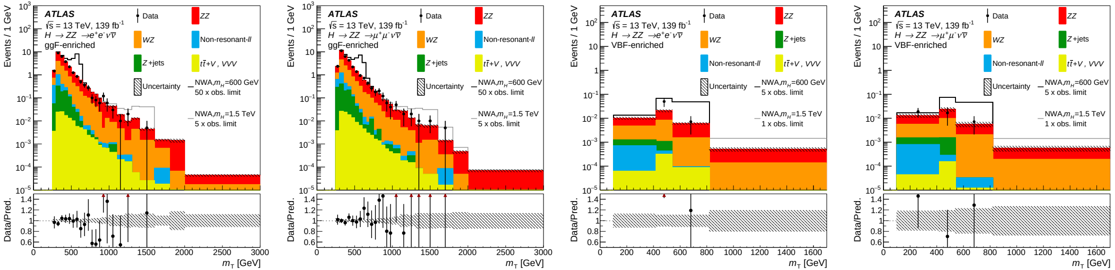

Combined Results

Combined Results

- Combine 4ℓ and $\ell\ell\nu\nu$ channels: **no significant excess observed**.
  - → Set upper limits on $\sigma \times \mathrm{BR}(X \to ZZ)$.
- Narrow-width signals: fits for ggF and VBF processes done separately (while profiling the other process) to remain model independent, *i.e.* assume no relative production rate between the two.
- Large-width signals: consider ggF only for widths of 1 %, 5 %, 10 % and 15 % of m_H [see Backup].
- Interpretations also in 2HDM models and for a Randall-Sundrum graviton [see Backup].

EPJC **81** (2021) 332

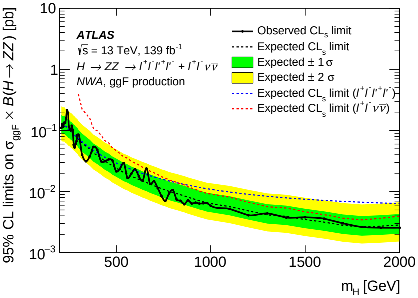

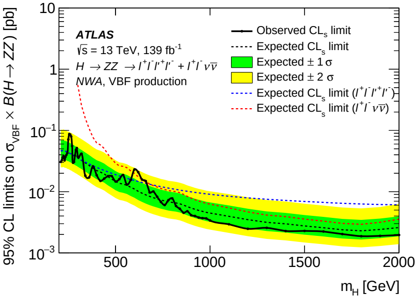

Upper Limits (95 % CL)

ggF:
- 200 fb at 240 GeV
- 2.6 fb at 2000 GeV

VBF:
- 87 fb at 250 GeV
- 1.9 fb at 1800 GeV

Combined Results

- Combine 4ℓ and $\ell\ell\nu\nu$ channels: **no significant excess observed**.
  - → Set upper limits on $\sigma \times \mathrm{BR}(X \to ZZ)$.
- Narrow-width signals: fits for ggF and VBF processes done separately (while profiling the other process) to remain model independent, *i.e.* assume no relative production rate between the two.
- Large-width signals: consider ggF only for widths of 1 %, 5 %, 10 % and 15 % of m_H [see Backup].
- Interpretations also in 2HDM models and for a Randall-Sundrum graviton [see Backup].

EPJC **81** (2021) 332

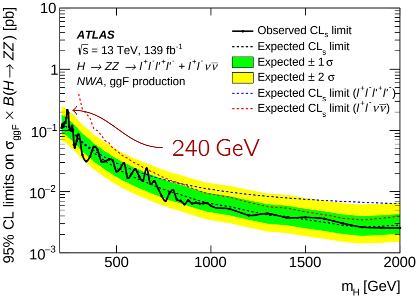

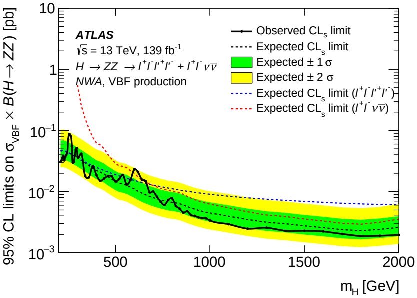

Upper Limits (95 % CL)

ggF:

- 200 fb at 240 GeV
- 2.6 fb at 2000 GeV

VBF:

- 87 fb at 250 GeV
- 1.9 fb at 1800 GeV

Combined Results

- Combine 4ℓ and $\ell\ell\nu\nu$ channels: **no significant excess observed**.
  - → Set upper limits on $\sigma \times \mathrm{BR}(X \to ZZ)$.
- Narrow-width signals: fits for ggF and VBF processes done separately (while profiling the other process) to remain model independent, *i.e.* assume no relative production rate between the two.
- Large-width signals: consider ggF only for widths of 1 %, 5 %, 10 % and 15 % of m_H [see Backup].
- Interpretations also in 2HDM models and for a Randall-Sundrum graviton [see Backup].

EPJC **81** (2021) 332

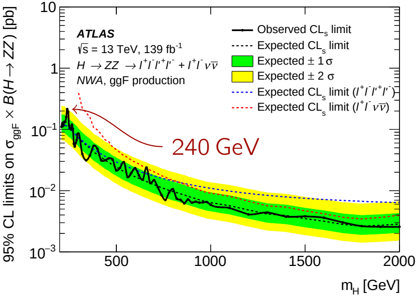

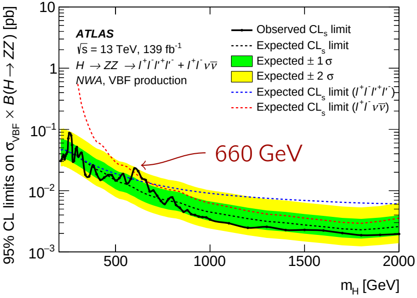

Upper Limits (95 % CL)

ggF:
- 200 fb at 240 GeV
- 2.6 fb at 2000 GeV

VBF:
- 87 fb at 250 GeV
- 1.9 fb at 1800 GeV

Summary

No significant excess over SM predictions

- ATLAS has an active BSM-Higgs and diboson-resonance search program, with many new results using the full Run 2 dataset, *e.g.:*
  - → $H \to \gamma\gamma$: arXiv 2102.13405
  - → $H^{\pm} \to tb$: arXiv 2102.10076
  - → $H^{\pm\pm} \to W^{\pm}W^{\pm}$: arXiv 2101.11961
- No new physics observed, but substantial update of constraints on 2HDM and other BSM models.
- Only small subset of results shown today: still many exciting new regions of phase space to probe using the full Run 2 dataset and beyond in LHC Run 3 (2022–2024) and at the high-luminosity LHC.

Latest ATLAS results at `https://twiki.cern.ch/twiki/bin/view/AtlasPublic`

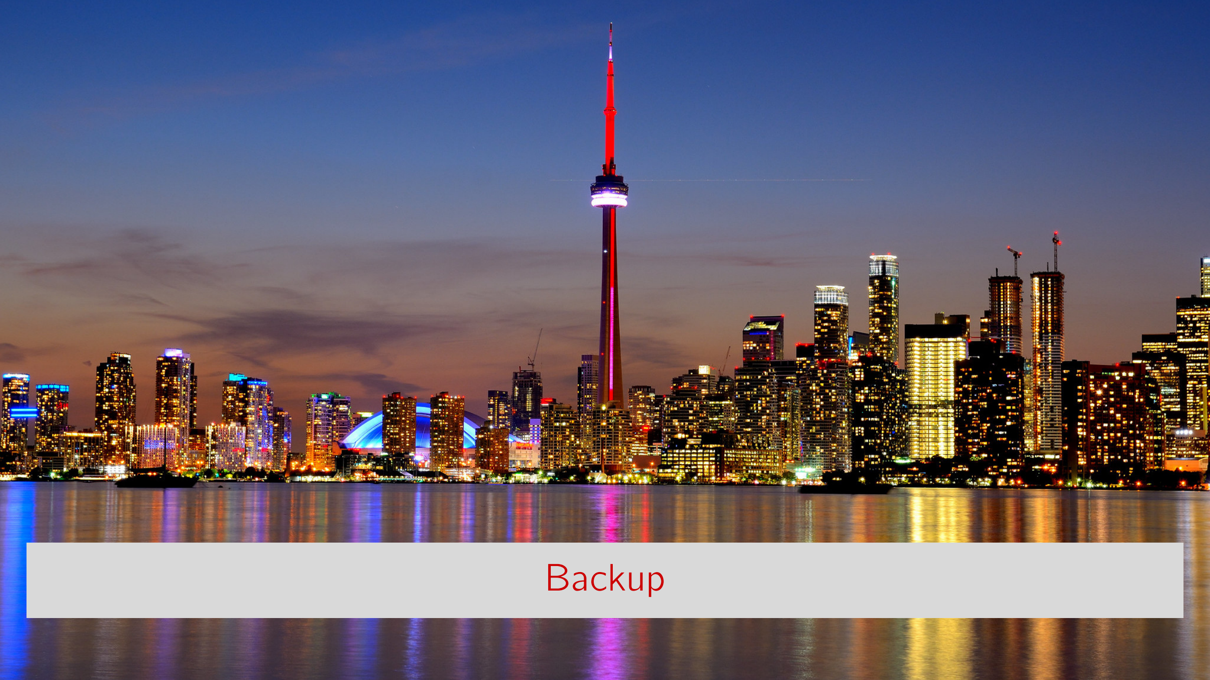

Backup

DNN inputs for the 4ℓ classifier

HIGG-2018-09

Input features used in the **VBF** (left) and the **ggF** (right) classifiers. 'rNN' stands for the recurrent neural network and 'MLP' for the multilayer perceptron.

VBF classifier

Model	Inputs	Description
rNN	p_T^{j0}, p_T^{j1}	transverse momenta of the two leading jets
	η^{j0}, η^{j1}	pseudorapidity of the two leading jets
	$p_T^{\ell 0}, p_T^{\ell 1}, p_T^{\ell 2}, p_T^{\ell 3}$	transverse momenta of the four leptons
	$\eta^{\ell 0}, \eta^{\ell 1}, \eta^{\ell 2}, \eta^{\ell 3}$	pseudorapidity of the four leptons
MLP	$m_{4\ell}$	invariant mass of the four-lepton system
	m_{jj}	invariant mass of the two-leading-jet system
	p_T^{jj}	transverse momentum of the two-leading-jet system
	$\Delta\eta_{H,j}$	difference in pseudorapidity between the four-lepton system and the leading jet
	$\min\Delta R_{jZ}$	minimum distance between one of the two lepton pairs and a jet

ggF classifier

Model	Inputs	Description
rNN	$p_T^{\ell 0}, p_T^{\ell 1}, p_T^{\ell 2}, p_T^{\ell 3}$	transverse momenta of the four leptons
	$\eta^{\ell 0}, \eta^{\ell 1}, \eta^{\ell 2}, \eta^{\ell 3}$	pseudorapidity of the four leptons
MLP	$m_{4\ell}$	invariant mass of the four-lepton system
	$p_T^{4\ell}$	transverse momentum of the four-lepton system
	$\eta^{4\ell}$	pseudorapidity of the four-lepton system
	$\cos\theta^*$	production angle of the leading Z defined in the four-lepton rest frame
	$\cos\theta_1$	angle between the negative final state lepton and the direction of flight of leading Z in the Z rest frame
	$\cos\theta_2$	angle between the negative final state lepton and the direction of flight of sub-leading Z in the Z rest frame
	Φ	angle between the decay planes of the four final state leptons expressed in the four-lepton rest frame
	p_T^{j0}	transverse momentum of the leading jet
	η^{j0}	pseudorapidity of the leading jet

Additional 4ℓ results

HIGG-2018-09

$\ell^+\ell^-\ell^+\ell^-$ Distributions

- Distributions of the four-lepton invariant mass $m_{4\ell}$ in each of the five event categories in the $\ell^+\ell^-\ell^+\ell^-$ channel.

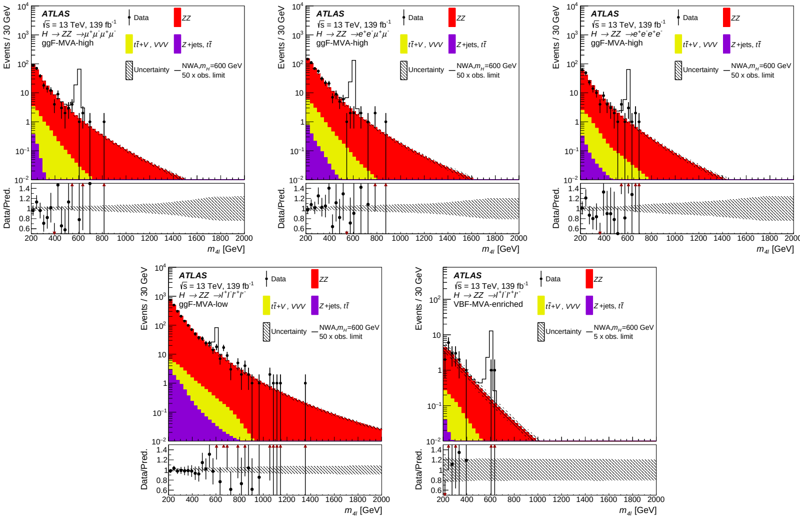

ZZ normalization factors

HIGG-2018-09

The ZZ normalisation factors together with their total uncertainties in each category of the two final states, which scale the number of ZZ events estimated from the simulations, obtained from a simultaneous likelihood fit of the two final states under the background-only hypothesis.

Final state	Normalisation factor	Fitted value
$\ell^+\ell^-\ell'^+\ell'^-$	$\mu_{ZZ}^{\text{VBF-MVA}}$	0.9 ± 0.3
	$\mu_{ZZ}^{\text{ggF-MVA-high}}$	1.07 ± 0.05
	$\mu_{ZZ}^{\text{ggF-MVA-low}}$	1.12 ± 0.03
$\ell^+\ell^-\nu\bar{\nu}$	μ_{ZZ}	1.07 ± 0.05

Additional combined results

HIGG-2018-09

Large-width spin-0 Interpretations

- 95 % CL upper limits on $\sigma_{\text{ggF}} \times \text{BR}(H \to ZZ)$ as a function of m_H assuming a width of 1, 5, 10 and 15 % of m_H.

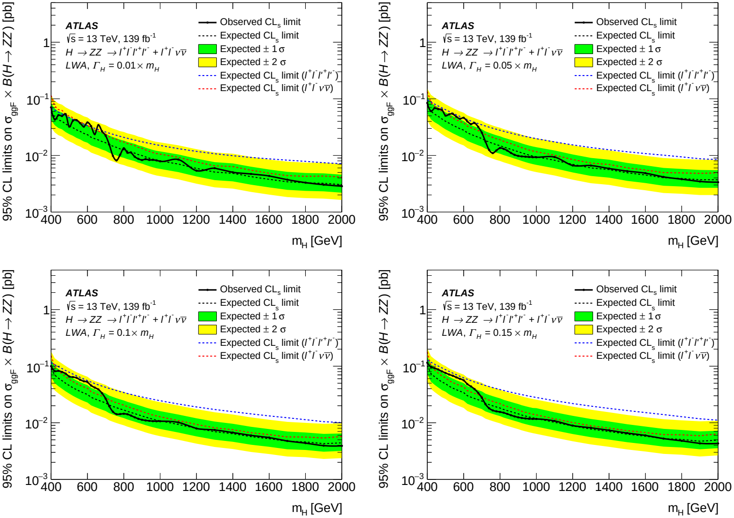

Additional combined results

HIGG-2018-09

2HDM Interpretations

- Exclusion contour in the Type-I and Type-II 2HDM models:
  - ➜ As a function of the parameters $\cos(\beta-\alpha)$ and $\tan\beta$, with $m_H = 220$ GeV
  - ➜ As a function of m_H and $\tan\beta$, with $\cos(\beta-\alpha) = -0.1$

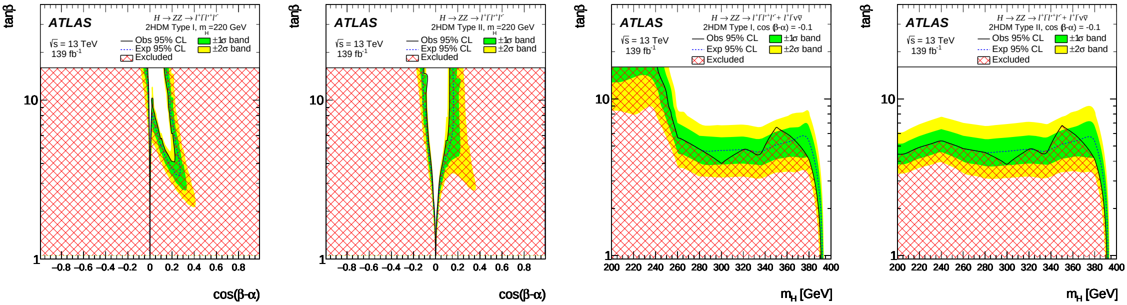

Additional combined results

HIGG-2018-09

RS Graviton Interpretations

- 95 % CL upper limits on $\sigma \times \mathrm{BR}(G_{\mathrm{KK}} \to ZZ)$ for a KK graviton produced with $k/\bar{M}_{Pl} = 1$.

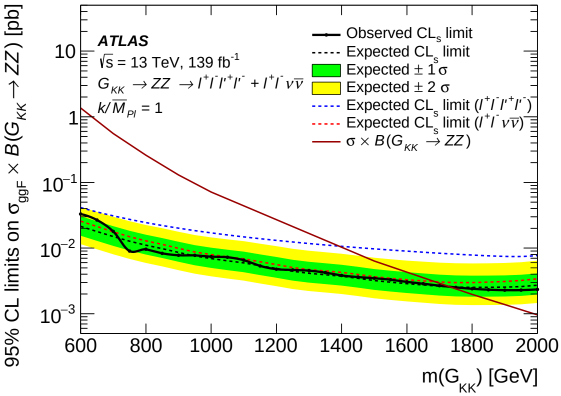

Uncertainties

HIGG-2018-09

Impact of the leading systematic uncertainties, the data statistical uncertainties and the total uncertainties on the predicted signal event yield with the cross section times branching ratio being set to the expected upper limit, expressed as a percentage of the signal yield:

ggF production: Systematic source	Impact [%]	VBF production: Systematic source	Impact [%]
$m_H = 300$ GeV			
ZZ parameterisation ($\ell^+\ell^-\ell'^+\ell'^-$)	4.5	Jet flavor composition	3.0
Z + jets modelling ($\ell^+\ell^-\nu\bar{\nu}$)	2.3	$q\bar{q} \to ZZ$ QCD scale (VBF-enriched category, $\ell^+\ell^-\ell'^+\ell'^-$)	2.8
Parton showering of ggF ($\ell^+\ell^-\ell'^+\ell'^-$)	2.2	ZZ parameterisation ($\ell^+\ell^-\ell'^+\ell'^-$)	2.3
$e\mu$ statistical uncertainty $\ell^+\ell^-\nu\bar{\nu}$	2.0	Jet energy scale(*in-su* calibration)	1.8
Data stat. uncertainty	53	Data stat. uncertainty	58
Total uncertainty	55	Total uncertainty	60
$m_H = 600$ GeV			
Electroweak corrections for $q\bar{q} \to ZZ$ ($\ell^+\ell^-\nu\bar{\nu}$)	4.9	QCD scale of $q\bar{q} \to ZZ$ ($\ell^+\ell^-\nu\bar{\nu}$)	7.6
QCD scale of $q\bar{q} \to ZZ$ ($\ell^+\ell^-\nu\bar{\nu}$)	2.5	Jet energy resolution	5.4
Z + jets modelling ($\ell^+\ell^-\nu\bar{\nu}$)	2.5	Parton showering ($\ell^+\ell^-\nu\bar{\nu}$)	3.3
PDF of $q\bar{q} \to ZZ$ ($\ell^+\ell^-\ell'^+\ell'^-$)	2.2	Electroweak corrections for $q\bar{q} \to ZZ$ ($\ell^+\ell^-\nu\bar{\nu}$)	3.0
Data stat. uncertainty	54	Data stat. uncertainty	61
Total uncertainty	57	Total uncertainty	63
$m_H = 1000$ GeV			
Electroweak corrections for $q\bar{q} \to ZZ$ ($\ell^+\ell^-\nu\bar{\nu}$)	9.3	Parton showering ($\ell^+\ell^-\nu\bar{\nu}$)	6.8
Parton showering ($\ell^+\ell^-\nu\bar{\nu}$)	5.2	Electroweak corrections for $q\bar{q} \to ZZ$ ($\ell^+\ell^-\nu\bar{\nu}$)	4.7
QCD scale of $q\bar{q} \to ZZ$ ($\ell^+\ell^-\nu\bar{\nu}$)	4.8	QCD scale of $q\bar{q} \to ZZ$ ($\ell^+\ell^-\nu\bar{\nu}$)	2.4
Z + jets modelling ($\ell^+\ell^-\nu\bar{\nu}$)	2.4	Jet flavor composition	2.4
Data stat. uncertainty	57	Data stat. uncertainty	58
Total uncertainty	59	Total uncertainty	59
$m_H = 1500$ GeV			
Parton showering ($\ell^+\ell^-\nu\bar{\nu}$)	9.6	Parton showering ($\ell^+\ell^-\nu\bar{\nu}$)	9.0
Electroweak corrections for $q\bar{q} \to ZZ$ ($\ell^+\ell^-\nu\bar{\nu}$)	6.8	Electroweak corrections for $q\bar{q} \to ZZ$ ($\ell^+\ell^-\nu\bar{\nu}$)	4.6
PDF of $q\bar{q} \to ZZ$ ($\ell^+\ell^-\nu\bar{\nu}$)	5.4	PDF of $q\bar{q} \to ZZ$ ($\ell^+\ell^-\nu\bar{\nu}$)	3.4
QCD scale of $q\bar{q} \to ZZ$ ($\ell^+\ell^-\nu\bar{\nu}$)	4.6	QCD scale of $q\bar{q} \to ZZ$ ($\ell^+\ell^-\nu\bar{\nu}$)	2.8
Data stat. uncertainty	57	Data stat. uncertainty	55
Total uncertainty	59	Total uncertainty	57

Expected and observed event yeilds

HIGG-2018-09

Expected and observed numbers of events in the 4ℓ final state for $m_{4\ell} > 200$ GeV (top) and the $\ell\ell\nu\nu$ final state (bottom). The expected numbers of events, as well as their uncertainties, are obtained from a combined likelihood fit to the data under the background-only hypothesis. The uncertainties of the ZZ normalisation factors are also taken into account.

4ℓ

Process	VBF-enriched	ggF-MVA-high 4μ channel	ggF-MVA-high 2e2μ channel	ggF-MVA-high 4e channel	ggF-MVA-low
$q\bar{q} \to ZZ$	11 ± 4	232 ± 10	389 ± 17	154 ± 7	2008 ± 47
$gg \to ZZ$	3 ± 2	37 ± 6	64 ± 10	26 ± 4	247 ± 19
ZZ (EW)	4.1 ± 0.4	4.5 ± 0.2	7.5 ± 0.4	3 ± 0.2	14.3 ± 0.7
Z + jets, $t\bar{t}$	0.08 ± 0.02	0.6 ± 0.1	1.7 ± 0.4	0.8 ± 0.1	8.8 ± 2.1
$t\bar{t}V$, VVV	0.97 ± 0.1	9.8 ± 0.2	17.5 ± 0.4	7.8 ± 0.2	21.9 ± 0.5
Total background	19 ± 5	284 ± 12	480 ± 20	192 ± 8	2300 ± 51
Observed	19	271	493	191	2301

$\ell\ell\nu\nu$

Process	ggF-enriched e^+e^- channel	ggF-enriched $\mu^+\mu^-$ channel	VBF-enriched e^+e^- channel	VBF-enriched $\mu^+\mu^-$ channel
$q\bar{q} \to ZZ$	714 ± 38	817 ± 44	2.9 ± 0.2	3.5 ± 0.2
$gg \to ZZ$	94 ± 29	105 ± 32	1 ± 0.5	1 ± 0.4
ZZ (EW)	6.6 ± 0.5	7 ± 0.5	0.8 ± 0.1	0.9 ± 0.1
WZ	412 ± 14	455 ± 12	2.5 ± 0.5	3 ± 1.5
Z + jets	43 ± 13	60 ± 22	0.3 ± 0.2	0.4 ± 0.3
Non-resonant-$\ell\ell$	66 ± 6	77 ± 7	0.2 ± 0.2	0.3 ± 0.2
$t\bar{t}V$, VVV	5.9 ± 0.4	5.9 ± 0.4	0.09 ± 0.02	0.04 ± 0.01
Total backgrounds	1342 ± 52	1527 ± 60	7.8 ± 0.8	9 ± 1.6
Observed	1323	1542	8	10

Analysis improvements

HIGG-2018-09

- Improvements on the expected 95 % CL upper limits w.r.t. previous and cut-based analyses for the **ggF** production mode (left) and the **VBF** production mode (right).

ggF

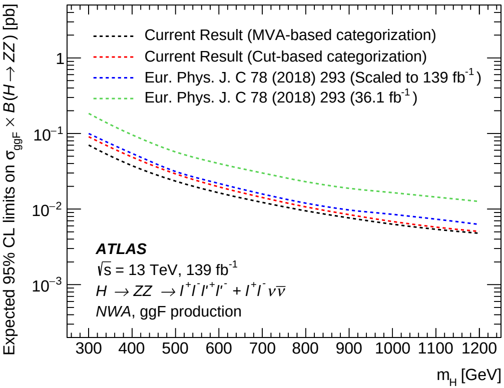

VBF